

Medium Access for Multi-Cell ISAC Through Scheduling of Radar and Communication Tasks

João Henrique Inacio de Souza*, Fabio Saggese†, Kun Chen-Hu‡, Petar Popovski*

*Department of Electronic Systems, Aalborg University, Denmark. E-mail: {jhids,petarp}@es.aau.dk

†Department of Information Engineering, University of Pisa, Italy. E-mail: fabio.saggese@ing.unipi.it

‡Department of Signal Theory and Communications, Universidad de Alcalá, Spain. E-mail: kun.chen@uah.es

Abstract—This paper focuses on communication, radar search, and tracking task scheduling in multi-cell integrated sensing and communication (ISAC) networks under quality-of-service constraints. We propose a medium access control framework that multiplexes these tasks while optimizing radar scan patterns through an interference-aware scheduling algorithm. Specifically, the proposed framework employs time-domain task scheduling and beam selection, formulated as an assignment problem, to mitigate inter-task and inter-cell interference, respectively. Simulations show that our solution guarantees target communication throughput, sensing target detection probability, and sensing signal-to-interference-plus-noise ratio with improved resource efficiency over baseline schemes, highlighting the benefits of coordinated scheduling in multi-cell ISAC.

Index Terms—Integrated sensing and communication, space-division multiple access, resource management, interference.

I. INTRODUCTION

The vision for the sixth generation of mobile networks (6G) centers on *connected intelligence*, by, among other solutions, seamlessly blending communication and localization [1]. This redefines the traditional role of a base station (BS), as it now serves both to support digital links as well as interface the physical world through radar probes. By unifying these functions into one transmitter–receiver platform, integrated sensing and communication (ISAC) eliminates redundant infrastructure and can achieve tighter performance synergies than independent radar and communication systems [2].

Most ISAC research to date has focused on waveform design to guarantee a certain quality of service (QoS) in terms of communication throughput and sensing metrics, such as range resolution, Doppler tolerance, and angular discrimination [3]. Efforts at higher layers have looked at joint resource allocation strategies—time-frequency partitioning, multiple access, and power control—that balance the conflicting demands of radar and data traffic in single-cell environments, *e.g.*, [4], [5]. A more recent strand of work has introduced the notion of a cooperative ISAC network, in which multiple sensing-capable BSs coordinate their transmissions and jointly process echoes [2]. Such an approach can significantly improve detection coverage, suppress mutual interference,

The work by J. H. Inacio de Souza and P. Popovski was supported by the Villum Investigator Grant “WATER” from the Velux Foundation, Denmark. The work by F. Saggese was supported by the Horizon Europe MSCA Postdoctoral Fellowships with Grant 101204088. The work by K. Chen-Hu was supported by the Ramón y Cajal Programme under Grant RYC2024-048736-I funded by MICIU/AEI/10.13039/501100011033 and FSE+.

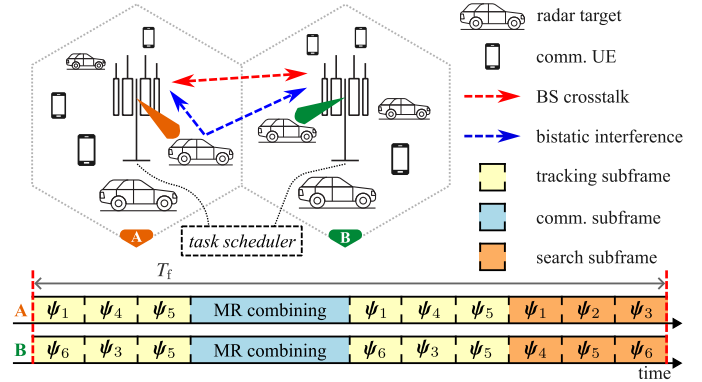


Figure 1. Multi-cell sensing and communication network and proposed frame design for task coexistence. During the tracking and search subframes, BSs transmit radar pulses with the beamforming vectors $\psi_j \in \Psi_i$. During the communication subframe, BSs employ MR combining to receive UEs’ data.

and refine localization accuracy by fusing observations from diverse viewpoints [6], [7].

A viable approach enabling cooperative ISAC is exploiting the current multi-cell infrastructure. Localization performance typically benefits from wide bandwidths, which, under conventional cellular planning, implies full frequency reuse across neighboring cells. Unfortunately, this also amplifies radar-to-radar interference, which in turn may eventually degrade radar performance instead of enhancing it [8]. What is thus needed is a space-time spectrum sharing strategy that orchestrates when and where each BS performs sensing and communication, so as to localize radar targets without sacrificing users equipment (UEs) QoS. On this line, recent works have focused on beamforming design for multiple-input multiple-output (MIMO) BSs. The authors of [7] and [9] proposed beamforming optimization to maximize sensing coverage in a multi-BS, single-cell environment, and to mitigate inter-cell interference in multi-cell ISAC systems, respectively. [10] focuses on a multi-BS beamforming design able to exploit shared channel state information (CSI) and data among BSs to enable bistatic sensing between cells. [11] extends the beamforming design to multi-array BSs and transmit/receive mode selection, maximizing the sensing signal-to-interference-plus-noise ratio (SINR) subject to communication SINR constraints.

From the medium access control (MAC) layer perspective, scheduling for multi-cell ISAC remains underexplored.

Moreover, sensing itself entails heterogeneous tasks—*search*, which scans wide areas for new objects, and *tracking*, which allocates resources to monitor known targets with high precision [12]. A practical framework must thus allocate resources not only across cells but also between these sensing modes, while safeguarding minimum data rate guarantees. This challenge reduces to designing a multi-cell MAC framework that dynamically orchestrates shared space–time resources for communication and radar tasks. In this work, we propose a MAC layer framework where communication and sensing are time multiplexed, enabling a tractable optimization of search, tracking, and data transmission tasks. Specifically, the proposed framework employs time-domain task scheduling and beam selection—formulated as an assignment problem—to mitigate inter-task and inter-cell interference, respectively. Then, communication and radar tasks are scheduled to satisfy communication throughput, sensing target detection, and sensing SINR. Our approach jointly coordinates cells to achieve improved sensing–communication coexistence with efficient resource utilization. Simulations prove that the proposed framework satisfies radar requirements with reliability above 0.999, outperforming the baselines.

II. SYSTEM MODEL

We analyze a multi-cell scenario comprised of a cluster of N_c cells with radius R , each having a BS at its center, as shown in Fig. 1. The overall bandwidth available for the cluster is W , while the carrier wavelength is denoted by λ . The BSs are equipped with uniform linear arrays (ULAs) of N_a half-wavelength spaced antennas lying in the xy -plane (parallel to the ground). In each cell, the BS aims to perform communication towards UEs while performing radar operations, which comprises *search* and *tracking* tasks, further described in Sec. III-B. Finally, communication and radar tasks are assumed to be multiplexed in the time domain, as detailed in Sec. III, to neglect the inter-task interference generated and study the fundamental trade-offs between communication, search, and tracking.

a) Communication model: We consider the uplink (UL) direction of a multi-cell massive MIMO system employing frequency reuse factor 1, *i.e.*, all UEs share the same frequency resources [13]. BS i has a set \mathcal{L}_i of UEs to serve. At the start of the communication operations, the CSI is acquired through standard pilot-based methods. To present a simple communication metric for the trade-off analysis, we assume uncorrelated Rayleigh fading, no occurrence of pilot contamination, and adoption of MR combining. Accordingly, the effective UL SINR of user $l \in \mathcal{L}_i$ in cell i results in [13, Theo. 4.4]

$$\gamma_{il} = \frac{N_a p_c \beta_{il}^i}{N_0 W + \sum_{j=1}^{N_c} \sum_{k \in \mathcal{L}_j} p_c \beta_{jk}^i - p_c \beta_{il}^i}, \quad (1)$$

where p_c is the transmit power, β_{jk}^i is the large-scale fading coefficient of the k -th UE of cell j to BS i , and N_0 is the noise power spectral density.

b) Radar model: All cells in the system employ the full available system bandwidth W for radar operations, generating inter-cell radar interference [1]. Let us evaluate the average SINR of the echo reception considering a single radar pulse transmission with power p_r and a generic target k , which position is described by the range ρ_{ik} and azimuth $\theta_{ik} \in [-\pi, \pi)$, both defined w.r.t. the position of BS i . To characterize the target reflectivity, we consider a Swerling 1 model with σ_{ij} being the target radar cross-section (RCS) when BS j transmits and the BS i receives. For $i = j$, the σ_{ij} is the monostatic RCS, while it is bistatic for $i \neq j$. Moreover, the following assumption holds.

Assumption 1. *The impinging signals in the radar receiver are modeled as independent, memoryless Gaussian sources.*

The BSs use beamforming at their ULAs for pulse transmission and echo reception. In this regard, $\phi_i \in \mathbb{C}^{N_a}$ is the beamforming vector of BS i . We further denote by $\Psi_i = \{\psi_j\}_{j=1}^{N_1}$, with $\psi_j \in \mathbb{C}^{N_a}$ and $N_1 = |\Psi_i|$, the *beamforming codebook*, *i.e.*, the set of beamforming vectors available to BS i , designed to provide the minimum number of configurations able to probe the whole coverage area with sufficient power, see, *e.g.*, [10]. Assuming far-field propagation for all the points in space relevant to the analysis, we denote as $G(\theta; \phi_i)$ the array power pattern for a signal traveling to or from azimuth angle θ w.r.t. BS i loading beamforming vector $\phi_i \in \Psi_i$.

From the *radar range equation*, the average received power by BS i resulted from the scattering from target k while employing beamformer ϕ_i is [14]:

$$M_{ik}(\phi_i) = \frac{p_r G(\theta_{ik}; \phi_i)^2 \lambda^2 \sigma_{ik}}{(4\pi)^3 \rho_{ik}^4}, \quad (2)$$

referred to as the received *monostatic power*.

The interference provoked by BS j on BS $i \neq j$ can be described by two components. The first one arises when the transmit and receive array power gain of the two BSs are simultaneously nonzero, *i.e.*, $G(\theta_{ik}; \phi_i) \neq 0$ and $G(\theta_{jk}; \phi_j) \neq 0$ for some k . This component is referred to as the received *bistatic interference power*, defined as [14]:

$$B_{ijk}(\phi_i, \phi_j) = \frac{p_r G(\theta_{jk}; \phi_j) G(\theta_{ik}; \phi_i) \lambda^2 \sigma_{ij}}{(4\pi)^3 \rho_{jk}^2 \rho_{ik}^2}. \quad (3)$$

The second component arises when the transmit and receive array power gain of the two BSs are simultaneously nonzero for the directions of each other, *i.e.*, $G(\vartheta_{ij}; \phi_i) \neq 0$ and $G(\vartheta_{ji}; \phi_j) \neq 0$, where $\vartheta_{ij} \in [-\pi, \pi)$ is the azimuth of BS j w.r.t. the position of BS i , and vice versa. We name it the received *BS crosstalk power*, resulting in:

$$C_{ij}(\phi_i, \phi_j) = \frac{p_r G(\vartheta_{ij}; \phi_i) G(\vartheta_{ji}; \phi_j) \lambda^2}{(4\pi)^2 \varrho_{ij}^2}, \quad (4)$$

where ϱ_{ij} is the distance between BS j and BS i .

We define the set \mathcal{K} containing the indices of the targets in the area covered by the cluster. Additionally, let $\phi = [\phi_1^T \cdots \phi_{N_c}^T]^T$ be the vector collecting the beamformers set

$$\Gamma_{ik}(\boldsymbol{\phi}) = M_{ik}(\boldsymbol{\phi}_i) \left(N_0W + \sum_{\substack{k' \in \mathcal{K} \\ k' \neq k}} M_{ik'}(\boldsymbol{\phi}_i) + \sum_{\substack{j=1 \\ j \neq i}}^{N_c} \sum_{k \in \mathcal{K}} B_{ijk}(\boldsymbol{\phi}_i, \boldsymbol{\phi}_j) + \sum_{\substack{j=1 \\ j \neq i}}^{N_c} C_{ij}(\boldsymbol{\phi}_i, \boldsymbol{\phi}_j) \right)^{-1}, \quad (5)$$

by all BSs. Thus, using eqs. (2), (3), and (4), we obtain the received SINR of target k 's echo as a function of $\boldsymbol{\phi}$ as in eq. (5) at the top of the page, where N_0W is the noise power.¹ The received communication SINR in (1) and radar SINR in (5) are used to evaluate the communication and radar performances.

III. RADAR AND COMMUNICATION COEXISTENCE

Here, we describe the communication and radar tasks performed by the network. To perform a space-time resource sharing strategy, the BSs operations are synchronized following a shared frame-based structure² of duration T_f , shown at the bottom of Fig. 1. In each frame, each task occupies a specific subframe, namely T_c for communication, T_s for search, and T_t for tracking; this results in a total duration of $T_f = T_c + T_s + T_t$. Each BS can execute only a single task at a time.

A. Communication Task

The communication task comprises the reception of UL data from the UEs in a cell. Each BS executes only one communication task per frame, and throughput is the QoS metric used to evaluate performance. According to eq. (1), the network throughput is lower bounded by [13]

$$S = \frac{T_c}{T_f} W \sum_{i=1}^{N_c} \sum_{l \in \mathcal{L}_i} \log_2(1 + \gamma_{il}). \quad (6)$$

Eq. (6) shows the direct relation between throughput and duration of the communication subframe.

B. Radar Tasks

Each BS performs search and tracking radar tasks. The former focuses on the discovery of new targets, while the latter focuses on tracking parameters of already discovered targets.

a) Search task: At this stage, the BS has no prior information about the potential targets' positions, so it needs to scan the entire cell area to identify them. Each search task configures a *detection problem*, which is defined as a *hypothesis testing* based on the echoes of N_p radar pulses transmitted when the BSs employ beamforming vectors to probe specific directions. To complete a single probe, the transmission of N_p pulses takes T_d seconds, that is, T_d is the radar dwell time.

The search performance is evaluated through the *probability of target detection*. According to Assumption 1 and that

$N_p \Gamma_{ik}(\boldsymbol{\phi}) > 1$, the probability of BS i detecting target k can be approximated as [14, eq. (6.99)]:

$$P_{ik}^d(\boldsymbol{\phi}) = \left(1 + \frac{1}{N_p \Gamma_{ik}(\boldsymbol{\phi})} \right)^{N_p - 1} \exp \left\{ \frac{-\tau}{1 + N_p \Gamma_{ik}(\boldsymbol{\phi})} \right\}, \quad (7)$$

where τ is the detection threshold, set according to the *probability of false alarm* given by $P^{\text{fa}} = 1 - I(\tau/\sqrt{N_p}, N_p - 1)$, where $I(\cdot, \cdot)$ denotes the incomplete Gamma function [14, eq. (6.80)]. Eq. (7) shows that the detection probability for a cell depends on the beamforming vectors loaded by all BSs, revealing the need for a joint selection of the beamformers from the respective codebooks to ensure a target performance.

To scan the whole network coverage area, the BSs need to execute a total of $N_c N_t$ searches. Given that, let $D_s \in [N_t, N_c N_t]$ denote the number of consecutive *dwell intervals* required to execute the task. Specifically, $D_s \leq N_c N_t$ may be achieved through a space-time sharing strategy, allowing BSs to execute searches within the same time-frequency resources. Importantly, depending on its duration T_s , the search subframe may not accommodate D_s dwell intervals, meaning that a single network scan will span multiple frames. The time performance of the search task is evaluated through the *search rate*, given by

$$R_s = \frac{T_s}{D_s T_d} \text{ [full scans/frame]}, \quad (8)$$

illustrating the relationship between the search subframe duration, the number of dwell intervals, and the radar dwell time.

b) Tracking task: The tracking task is performed towards targets that have already been detected to retrieve their sensing parameters, *e.g.*, precise range, Doppler, or angular direction. Since the search task acquired information on approximate target direction, *i.e.*, the one illuminated by the beamformer $\boldsymbol{\phi}_i$ for BS i , the scan of the tracking task can be limited to a smaller set of range bins and spatial angles. Let us assume each BS tracks N_t targets previously detected in its cell through search. Each tracking task obtains a snapshot of the sensing parameters from a single target. Based on a series of snapshots, each BS runs a track algorithm on its N_t targets, *e.g.*, a Kalman filter for tracking the trajectory of targets over time.

The performance of any estimation procedure strongly depends, among other factors, on the SINR of the echoes received from the radar pulses [1]. For this reason, we adopt the SINR in (5) to evaluate tracking performance without defining a specific method. To ensure that the error covariances of the targets' sensing parameters are bounded in the tracking algorithm, the BSs execute tracking tasks for each target at a fixed rate R_t , referred to as the *tracking update rate*. Let $D_t \in [N_t, N_c N_t]$ denote the number of tracking dwell intervals

¹The effect of clutter and reflectivity of UEs is neglected for simplicity of analysis and will be included in future works.

²The control signaling burden between the BSs for a precise synchronization is left for future studies.

required for BSs to probe all targets. Then, the duration of the tracking subframe is calculated as

$$T_t = \lfloor T_f R_t \rfloor D_t T_d, \quad (9)$$

where $\lfloor T_f R_t \rfloor$ indicates the number of times a BS needs to revisit a target within a frame. Note that, as $T_t \leq T_f$, the number of targets that can be tracked and the rate at which they can be updated are limited. Eq. (9) is adopted to evaluate the time performance of the tracking tasks, and links the tracking subframe to the frame duration, the tracking update rate, the number of tracked targets, and the radar dwell time.

IV. TASK SCHEDULING STRATEGY

In this section, we introduce a task scheduling strategy with two objectives: 1) find BSs' scan patterns, *i.e.*, the selection of beamforming vector from the codebook, guaranteeing the radar operational requirements by mitigating inter-cell interference; and, 2) allocate time for communication, search, and tracking subframes to improve resource efficiency. The proposed strategy comprises a three-step algorithm that obtains the radar scan patterns and subframe allocation in order of task priority [12]. The proposed solution works regardless of the priority order chosen, which depends on the operational requirements. Here, we set tracking to be the highest priority because of its time sensitivity, as delayed probing may cause large estimation errors; then, communication follows to ensure a minimal level of radar-communication coexistence under resource constraints; search has the lowest priority.

The operational requirements of each task are: for tracking, each BS must probe all N_t targets $\lfloor T_f R_t \rfloor$ times per frame, receiving echo signals with a target SINR of $\bar{\Gamma}$; for communication, the network must achieve a throughput no less than \bar{S} ; for search, each BS must scan the entire cell area with detection probability at least \bar{P}^d . Thus, $(N_t, R_t, \bar{\Gamma}, \bar{S}, \bar{P}^d)$ form the inputs to the task scheduling algorithm.

A. Tracking Task Scheduling

To schedule the tracking tasks, the BSs' scan pattern and the subframe duration required to probe all the tracked targets must be determined. To this end, we formulate the optimization of the tracking scan pattern to minimize the number of dwell intervals, subject to the radar SINR constraint.

Let $\phi^{(d)} \in \mathbb{C}^{N_c N_a}$ denote the beamformers set by all BSs at the dwell interval d , and let $\Phi_t = \{\phi^{(d)}\}_{d=1}^{D_t}$ denote the tracking scan pattern. For BS i , let $\Psi'_i \subseteq \Psi_i$ be the set of beamformers used to probe its N_t tracked targets. We also define ψ_0 as the null beamforming vector, indicating that a BS does not transmit radar signals during a dwell interval.

Optimizing the beamformers w.r.t. the radar SINR in (5) requires knowledge of the interference terms, which depend on the locations of both detected and undetected targets. Since this is impractical, we introduce *virtual scatterers* to estimate the SINR of received radar signals.

Definition 1 (Virtual Scatterers). *For each cell and beamformer, a virtual scatterer is placed at the cell edge and*

aligned with a beamformer's half-power beamwidth. The set of virtual scatterers in cell i is denoted by \mathcal{K}_i , with $\bigcup_{i=1}^{N_c} \mathcal{K}_i = \mathcal{K}$ and $\mathcal{K}_i \cap \mathcal{K}_j = \emptyset, \forall i \neq j$. As such, $f_i : \Psi_i \rightarrow \mathcal{K}_i$ is a mapping of each beamformer to its corresponding virtual scatterer.

Based on Def. 1, the SINR of the radar signal received by BS i is $\Gamma_{i f_i(\phi)}(\phi)$, and the tracking scan pattern can be optimized by solving the following problem:

$$\underset{\Phi_t}{\text{minimize}} \quad D_t = |\Phi_t| \quad (10a)$$

$$\text{subject to} \quad \Gamma_{i f_i(\phi^{(d)})}(\phi^{(d)}) \geq \bar{\Gamma}, \quad \forall i, d, \quad (10b)$$

$$\bigcup_{d=1}^{D_t} \{\phi_i^{(d)}\} \setminus \{\psi_0\} = \Psi'_i, \quad \forall i, \quad (10c)$$

$$\{\phi_i^{(d)}\} \cap \{\phi_i^{(d')}\} \setminus \{\psi_0\} = \emptyset, \quad \forall i, d \neq d'. \quad (10d)$$

Constraint (10b) enforces the radar target SINR, while constraints (10c) and (10d) ensure that the scan pattern contains all beamformers required by the BSs, and that each appears only once, except for ψ_0 .

For small network configurations, (10) can be solved by enumeration. However, the number of potential solutions grows as $N_t^{N_c} / (N_t^{N_c} - D_t)!$ for a fixed D_t . To prove the effectiveness of the optimization in multi-cell scenarios, we propose a solution to (10) for the scenario with $N_c = 2$.³ This solution reformulates the original problem as an instance of the assignment problem, allowing efficient computation of the optimal scan pattern with standard solvers, even for large N_t .

Solution of (10) for two cells: Let the *multisets*⁴ with the indices of the beamformers of the two BSs be initialized as $\mathcal{U} \leftarrow \{u : \psi_u \in \Psi'_1\}$ and $\mathcal{V} \leftarrow \{v : \psi_v \in \Psi'_2\}$. Then, we define a cost function that equals zero only when, using $\phi = [\psi_u^T \ \psi_v^T]^T$, the SINR constraints at both BSs are satisfied:

$$c(u, v) = \begin{cases} 0, & \text{if } \Gamma_{1 f_1(\psi_u)}(\phi) \text{ and } \Gamma_{2 f_2(\psi_v)}(\phi) \geq \bar{\Gamma}, \\ 1, & \text{otherwise.} \end{cases} \quad (11)$$

The problem of finding the matching beamformers indexed by \mathcal{U} and \mathcal{V} that minimize the total cost is formulated as

$$\underset{\{x_{uv} \in \{0,1\}\}_{u,v}}{\text{minimize}} \quad C = \sum_{u \in \mathcal{U}} \sum_{v \in \mathcal{V}} c(u, v) x_{uv} \quad (12a)$$

$$\text{subject to} \quad \sum_{v \in \mathcal{V}} x_{uv} = 1, \quad \forall u, \quad \sum_{u \in \mathcal{U}} x_{uv} = 1, \quad \forall v. \quad (12b)$$

This is the classical assignment problem, solvable in polynomial time by the Hungarian algorithm [16]. If the optimal total cost $C^* = 0$, then a matching of beamformers exists in which all the SINR constraints are met. Otherwise, one of the BSs must remain silent during one or more dwell intervals: thus, we update the multisets as $\mathcal{U} \leftarrow \mathcal{U} + \{0\}$ and $\mathcal{V} \leftarrow \mathcal{V} + \{0\}$, and solve (12) again. This process

³For $N_c > 2$, the scan pattern optimization can be formulated as a graph coloring problem [15]. In this formulation, the graph vertices represent the beamformers used by each BS, while the edges connect pairs of beamformers whose simultaneous use violates the SINR constraint in (10b).

⁴Multisets consist of mathematical objects in which elements may appear with multiplicity greater than one.

Algorithm 1: Scan pattern optimization for 2 cells.

input: Cost function c and beamformers' indices \mathcal{U}, \mathcal{V}
output: Optimized scan pattern Φ^*

- 1: $(\{x_{uv}^*\}_{\forall u,v}, C^*) \leftarrow \text{Hungarian_algorithm}\{(12)\}$
- 2: **if** $C^* > 0$ **then**
- 3: $\mathcal{U} \leftarrow \mathcal{U} + \{0\}, \mathcal{V} \leftarrow \mathcal{V} + \{0\}$ and go to line 1
- 4: **end if**
- 5: **return** $\Phi^* \leftarrow \{[\psi_u^T \ \psi_v^T]^T : x_{uv}^* = 1, \forall u, v\}$

repeats until $C^* = 0$. The optimized tracking scan pattern is then obtained from the solution $\{x_{uv}^*\}_{\forall u,v}$ of (12) as $\Phi_t^* = \{[\psi_u^T \ \psi_v^T]^T : x_{uv}^* = 1, \forall u, v\}$. Accordingly, the number of required dwell intervals is $D_t^* = |\Phi_t^*|$, and from (9), the tracking subframe duration is $T_t = \lfloor T_f R_t \rfloor D_t^* T_d$. The overall procedure is summarized in Algorithm 1, which has worst-case complexity $O(|\mathcal{U}|^4)$ with efficient implementations of the Hungarian algorithm [17]. Since the procedure starts with \mathcal{U} and \mathcal{V} containing only Ψ_1' and Ψ_2' , and introduces silent dwell intervals gradually, Φ_t^* is always a feasible solution to (10).

B. Communication Task Scheduling

The communication tasks are scheduled to ensure the network achieves the required throughput \bar{S} . According to (6), the communication subframe duration results in

$$T_c = \frac{\bar{S} T_f}{W} \left(\sum_{i=1}^{N_c} \sum_{l \in \mathcal{L}_i} \log_2(1 + \gamma_{il}) \right)^{-1}. \quad (13)$$

If the available time resources are insufficient, *i.e.*, $T_f - T_t < T_c$, the communication tasks are not scheduled. This occurs, *e.g.*, when the tracking tasks occupy most of the frame to follow many fast-moving targets, or for high throughput requirements.

C. Search Task Scheduling

For the search task, the BSs' scan pattern is optimized to minimize the number of dwell intervals while satisfying a detection probability constraint. Letting $\Phi_s = \{\phi^{(d)}\}_{d=1}^{D_s}$ denote the search scan pattern, the problem is formulated as

$$\underset{\Phi_s}{\text{minimize}} \quad D_s = |\Phi_s| \quad (14a)$$

$$\text{subject to} \quad P_{i f_i(\phi^{(d)})}^d(\phi^{(d)}) \geq \bar{P}^d, \quad \forall i, d, \quad (14b)$$

$$\bigcup_{d=1}^{D_s} \{\phi_i^{(d)}\} \setminus \{\psi_0\} = \Psi_i, \quad \forall i, \quad (14c)$$

$$\{\phi_i^{(d)}\} \cap \{\phi_i^{(d')}\} \setminus \{\psi_0\} = \emptyset, \quad \forall i, d \neq d'. \quad (14d)$$

This formulation mirrors (10), except that constraint (14b) replaces the SINR constraint (10b). The problem reduces to an assignment problem that can be efficiently solved for $N_c = 2$.

To solve (14) for two cells, the cost function (11) is redefined to be zero when both $P_{1 f_1(\psi_u)}^d(\phi)$ and $P_{2 f_2(\psi_v)}^d(\phi) \geq \bar{P}^d$. Then, running Algorithm 1 with initialization $\mathcal{U} \leftarrow \{u : \psi_u \in \Psi_1\}$ and $\mathcal{V} \leftarrow \{v : \psi_v \in \Psi_2\}$ yields the optimized scan pattern $\Phi_s^* = \{[\psi_u^T \ \psi_v^T]^T : x_{uv}^* = 1, \forall u, v\}$ with $D_s^* = |\Phi_s^*|$

Table I
SIMULATION PARAMETERS

| Parameter | Value |
|--------------------------------|--|
| Number of cells, radius | $N_c = 2, R = 100$ m |
| Bandwidth, carrier wavelength | $W = 10$ MHz, $\lambda = 50$ mm |
| Frame duration | $T_f = 1$ s |
| UEs per cell, transmit power | $ \mathcal{L}_i = 10, p_c = 23$ dBm |
| Dwell time, number of pulses | $T_d = 13.3$ ms, $N_p = 20$ |
| Radar operational requirements | $\bar{P}^d = 0.9, \bar{P}^{\text{fa}} = 10^{-6}, \bar{\Gamma} = 10$ dB |

dwell slots. The duration of the allocated search subframe is $T_s = \max\{T_f - T_t - T_c, 0\}$, and from (8), the resulting search rate is $R_s = T_s / (D_s^* T_d)$.

The three procedures described in Secs. IV-A, IV-B, and IV-C form the proposed scheduling algorithm, used by the task scheduler to determine the subframe allocation and radar scan patterns.

V. NUMERICAL RESULTS

In this section, we provide numerical results to investigate the performance trade-offs of the proposed task scheduling strategy. The parameter values for the simulations are in Table I. The transmit power budget for the radar tasks, p_r , is set to achieve the detection constraint (\bar{P}^d) or SINR constraint ($\bar{\Gamma}$) for all virtual scatterers in the absence of interference. For the communication task, the UEs' large-scale fading coefficients are calculated by $\log_{10} \beta_{jk}^i = -47.9 - 21 \log_{10} r_{jk}^i$, where r_{jk}^i is the distance from UE k of cell j to BS i . The beamforming codebook is built using the phased array approach and *Hamming weighting* with $N_a = 29$, having an array power pattern $G(\theta; \phi_i)$ given in [18, eq. (3.22)], normalized to have a total transmit power of p_r ; the half-power criterion is adopted to characterize the radar beamwidth. In this simplified setting, each beamforming vector corresponds to a single look direction.⁵

Two baselines are adopted for comparison with the proposed scan patterns for search and tracking. In the *in-phase scan pattern*, the BSs beamformers point to the same relative directions at the same time, while, in the *random scan pattern*, the BSs select the beamformers randomly and independently. Only for the tracking task, the proposed scan pattern is compared with the *orthogonal scan pattern*, where the BSs' probes are orthogonal in the time domain, resulting in $D_t = N_c N_t$.

Fig. 2 shows the search and tracking performance achieved by the different scan patterns and different N_t . The proposed pattern outperforms the baselines, guaranteeing $P_i^d(\phi)$ and $\Gamma_{ik}(\phi)$ to achieve the targets \bar{P}^d and $\bar{\Gamma}$, respectively, with high reliability (> 0.999). Conversely, the random pattern shows the worst performance, achieving values considerably lower than \bar{P}^d and $\bar{\Gamma}$ with high probability, due to excessive inter-cell interference. The performance degradation of the baselines is reduced when increasing N_t , since having more look directions decreases the likelihood of the BSs to simultaneously select

⁵The proposed algorithm for scan pattern optimization can be applied without loss of generalization to any beamforming codebook.

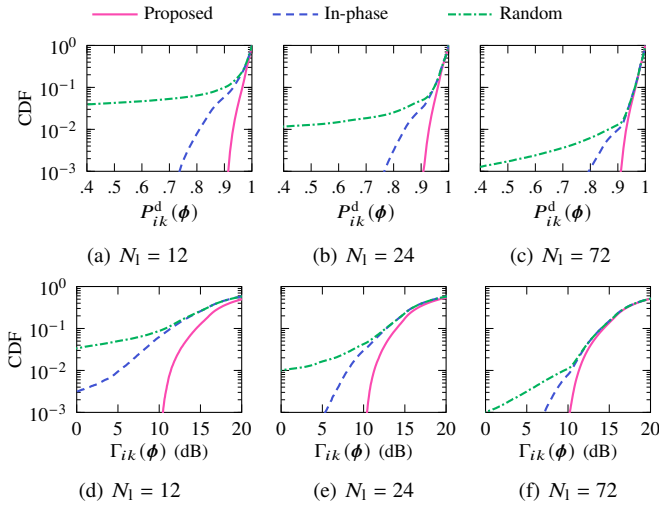
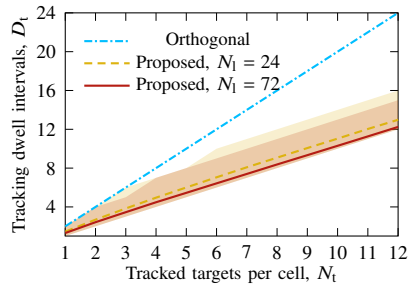


Figure 2. CDF of the detection probability, $P_{ik}^d(\phi)$, given by the search scan pattern and radar SINR, $\Gamma_{ik}(\phi)$, given by the tracking scan pattern. The proposed search pattern when $N_t = 12$ requires $D_s = 13$, so each BS needs to be turned off for one dwell interval. For all the other cases, $D_s = N_t$.

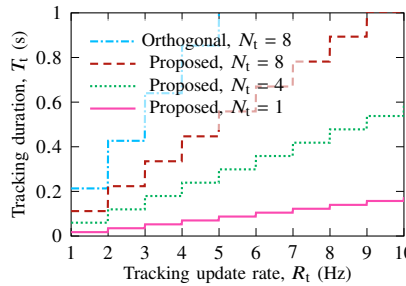
beamforming vectors with high interference. However, even with $N_t = 72$, the baselines cannot guarantee the target performance with a reliability higher than 0.99, which can only be achieved by the proposed patterns.

To investigate the tracking time performance, Fig. 3a depicts the average number of dwell intervals (lines) and the 99th percentile (shaded areas) obtained for different numbers of tracked targets per cell and look directions. Compared to the orthogonal scan pattern, the proposed approach achieves a remarkable reduction in the number of required dwell intervals both for $N_t = 24$ and $N_t = 72$, especially for high N_t . Moreover, when $N_t = 72$, the scan pattern achieves the minimum possible length on average, having as many dwell intervals as targets. Thus, the proposed tracking pattern requires fewer time resources, improving efficiency by leaving more of the frame for search and communication tasks.

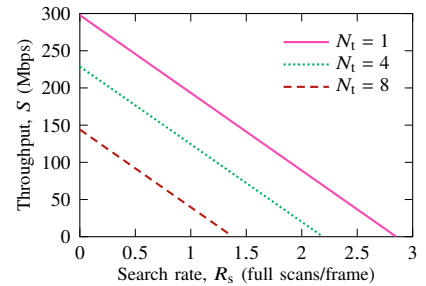
Fig. 3b shows the duration of the tracking subframe achieved by different scan patterns against the tracking update rate and by varying N_t . As expected, T_t grows with R_t and N_t due to the relation in eq. (9), and the increase of D_t



(a) Lines: average; shaded areas: 99th percentile.



(b) $N_t = 72$



(c) $N_t = 12$ (search) and 72 (tracking), $R_t = 5$ Hz

Figure 3. (a) Number of tracking dwell intervals required by the scan patterns vs. the number of tracked targets per cell. (b) Tracking subframe duration vs. the tracking update rate and number of tracked targets per cell. (c) Average communication throughput vs. the search rate and number of tracked targets per cell; the proposed patterns for search and tracking are adopted. All results are calculated over 10^4 realizations.

with N_t —see Fig. 3a. For $N_t = 8$, it is noticeable that the duration of the proposed pattern presents a lower slope than the orthogonal one. In this case, the orthogonal pattern limits R_t to 5 Hz before tracking occupies the entire frame of 1s, while the proposed pattern supports values up to 9 Hz. Hence, the proposed approach allows each BS to simultaneously track a larger number of moving targets whose positions change more often.

Fig. 3c shows the performance trade-offs of the tasks by showing the achievable region for communication throughput and search rate. The search and communication performance region degrades as N_t and R_t increase, as the longer tracking subframe, the fewer resources for the other tasks—see Fig. 3b.

VI. CONCLUSION

We proposed a scheduling strategy for multi-cell ISAC networks optimizing communication and radar task allocation. Results showed that our approach outperforms conventional baselines by ensuring reliable radar detection and tracking with fewer resources. The framework provides an efficient means of coordinating ISAC tasks at the MAC layer; future work will address scalability to larger networks and the impact of clutter.

REFERENCES

- [1] F. Liu et al., “Integrated sensing and communications: Toward dual-functional wireless networks for 6G and beyond,” *IEEE J. Sel. Areas Commun.*, vol. 40, no. 6, pp. 1728–1767, Jun. 2022.
- [2] K. Meng et al., “Cooperative ISAC networks: Opportunities and challenges,” *IEEE Wireless Commun.*, vol. 32, no. 3, pp. 212–219, Jun. 2025.
- [3] Z. Wei et al., “Integrated sensing and communication signals toward 5G-A and 6G: A survey,” *IEEE Internet Things J.*, vol. 10, no. 13, pp. 11 068–11 092, Jul. 2023.
- [4] F. Dong et al., “Sensing as a service in 6G perceptive networks: A unified framework for ISAC resource allocation,” *IEEE Trans. Wireless Commun.*, vol. 22, no. 5, pp. 3522–3536, May 2023.
- [5] D. Cao et al., “Joint optimization of computation offloading and resource allocation considering task prioritization in ISAC-assisted vehicular network,” *IEEE Internet Things J.*, vol. 11, no. 18, pp. 29 523–29 532, Sep. 2024.
- [6] S. Buzzi et al., “Scalability and implementation aspects of cell-free massive MIMO for ISAC,” in *Proc. Int. Symp. Wireless Commun. Syst. (ISWCS)*, Jul. 2024, pp. 1–6.
- [7] R. Li et al., “Toward seamless sensing coverage for cellular multi-static integrated sensing and communication,” *IEEE Trans. Wireless Commun.*, vol. 23, no. 6, pp. 5363–5376, Jun. 2024.

- [8] A. Munari et al., "Stochastic geometry interference analysis of radar network performance," *IEEE Commun. Lett.*, vol. 22, no. 11, pp. 2362–2365, Nov. 2018.
- [9] Z. Wang et al., "Interference mitigation in multi-cell ISAC systems: A three-dimensional MIMO precoding approach," *IEEE Commun. Lett.*, vol. 28, no. 11, pp. 2543–2547, Nov. 2024.
- [10] N. Babu et al., "Precoding for multi-cell ISAC: From coordinated beamforming to coordinated multipoint and bi-static sensing," *IEEE Trans. Wireless Commun.*, vol. 23, no. 10, pp. 14 637–14 651, Oct. 2024.
- [11] Q. Ma et al., "Multi-array beamforming and mode optimization for cooperative multi-cell ISAC systems," *IEEE Wireless Commun. Lett.*, vol. 14, no. 11, pp. 3480–3484, Nov. 2025.
- [12] A. Aubry et al., "A priority-based scheduling scheme for search, track, and communications in MPARs," *IEEE Transactions on Radar Systems*, vol. 2, pp. 471–481, Apr. 2024.
- [13] E. Björnson et al., "Massive MIMO networks: Spectral, energy, and hardware efficiency," *Found. Trends Signal Process.*, vol. 11, no. 3-4, pp. 154–655, 2017.
- [14] M. A. Richards, *Fundamentals of Radar Signal Processing*, 1st ed. New York, NY, USA: McGraw-Hill, 2005.
- [15] C. A. Floudas and P. M. Pardalos, Eds., *Encyclopedia of Optimization*, 2nd ed. New York, NY, USA: Springer, 2009.
- [16] H. W. Kuhn, "The Hungarian method for the assignment problem," *Naval research logistics quarterly*, vol. 2, no. 1-2, pp. 83–97, Mar. 1955.
- [17] J. Munkres, "Algorithms for the assignment and transportation problems," *J. of the Soc. for Ind. and Appl. Math.*, vol. 5, no. 1, pp. 32–38, Mar. 1957.
- [18] H. L. Van Trees, *Optimum Array Processing: Part IV of Detection, Estimation, and Modulation Theory*, 1st ed. New York, NY, USA: Wiley, 2002.